JOURNAL OF APPLIED ELECTROCHEMISTRY 11 (1981) 625–637

A preliminary investigation of some anodes for use in fluidized-bed electrodeposition of metals

D. P. ZIEGLER, M. DUBROVKSY, J. W. EVANS†

Department of Materials Science and Mineral Engineering, University of California, Berkeley, California 94720, USA

Received 19 November 1980

The development of fluidized-bed electrowinning for copper and other metals appears to be impeded by the high electrical energy consumption associated with the anodes used in such electrowinning. This paper describes preliminary work aimed at seeking anodes which consume less energy and are suitable for scale-up. Using laboratory-scale cells in which copper was electrowon from strong (25 g dm^{-3} Cu), acidified (100 g dm^{-3} H_2SO_4) sulphate solutions on to fluidized cathodes, the following anodes were tested: fluidized-bed anodes of catalyst-coated titanium particles, packed-bed anodes of lead shot and graphite, single and double layers of catalyst-coated titanium mesh, and cloth-covered anodes placed directly in the fluidized cathode. In addition, the possibility of using alternative anode reactions, namely oxidation of sulphur dioxide, ferrous ions or cuprous ions, as well as fluidized-bed electrowinning from a cuprous-ion catholyte, were examined. Except for the fluidized anode and the lead packed-bed anode, all the above systems yielded energy savings. The investigation was not sufficiently detailed to define which of the above was best, although, at 2.0 kW h kg^{-1} Cu, electrowinning from cuprous solutions with cuprous oxidation on a graphite packed-bed anode offered an energy consumption better than that of the conventional electrowinning plants.

1. Introduction

A number of investigations [1–8] into fluidized-bed electrodeposition of metals has been carried out; however, in these investigations the counter electrode has been a conventional anode, or one little different from conventional. It is not clear, *a priori*, that a conventional anode is the optimal one for commercial-scale, fluidized-bed electrowinning. Furthermore, many previous investigators have reported high cell voltages (i.e. high electrical energy consumptions) compared to conventional electrowinning; as will be seen below, this is likely to be due to the conventional anodes used in their cells, rather than to the fluidized cathode. A preliminary economic analysis [9] has indicated that, although attractive from a capital cost point of view, fluidized-bed electrowinning of copper would be economically inferior to conventional electrowinning if energy consumptions in the former were more than approximately 3.3 kW h kg^{-1} Cu. The objective of the present investigation was to discover superior anodes which would yield energy consumptions below this figure and thus be suitable for scale-up to a commercial cell.

Attention was restricted to electrowinning from strong (25 g dm^{-3} Cu), acidified (100 g dm^{-3} H_2SO_4) sulphate solutions, such as are produced by solvent extraction circuits, and cells of the 'side by side' configuration wherein anode and cathode compartments are separated by a diaphragm. Typical of investigations of such electrowinning is the work of Sabacky and Evans [10, 11] who have reported energy consumptions in the range 4.2 to 7.8 kW h kg^{-1} Cu. As a first step in the present investigation, an analysis was made of the voltage distribution within the cell for one of the runs (DP16) of Sabacky and Evans. The anode polarization was measured separately [12]; the anode chamber and diaphragm voltage drops were calculated by the application of Ohm's law,

† To whom correspondence should be addressed.

0021–891X/81/050625–13$03.30/0

Table 1. Base case cell voltage distribution

	Volts	*Percentage*
Reversible potential	0.89	14.3
Anode overpotential	0.51	8.2
Anolyte resistance loss	3.5	56.5
Diaphragm resistance loss	0.1	1.6
Cathode drop	1.2	19.4
Total	6.2	100.0

Corresponding energy consumption: 5.1 kW h kg^{-1} Cu

the resistivity of the electrolyte being corrected for the oxygen bubbles by use of Hine's correlation [13]. Table 1 shows the voltage distribution determined in this way. The anode chamber, a conventional one in the work of Sabacky and Evans, is seen to account for a large part of the cell voltage and, therefore, energy consumption. In fluidized-bed electrowinning, where superficial current densities (current per unit area of diaphragm) are typically over an order of magnitude greater than the current density of conventional electrowinning, the conventional anode is 'driven' too hard to yield reasonable energy consumption figures.

Further difficulties with the use of conventional anodes in fluidized-bed electrowinning exist. Masterson and Evans [14] have reported on the difficulties of adequately supporting the diaphragm is large (1000 A) cell and of avoiding a bypass phenomenon where catholyte flows through the diaphragm into the anode chamber at the bottom of the cell and back into the cathode chamber at the top of the cell. This bypassing defluidizes the cathode at the mid-height of the cell. Furthermore, any flow through the diaphragm is to be avoided in cells where catholyte and anolyte must be kept separate (although Masterson and Evans demonstrated that a small flow from anode to cathode chambers can be desirable in some circumstances). The problem arises from the differing bulk densities, resulting in different hydrostatic pressure gradients, on either side of the diaphragm. One solution, illustrated in Fig. 1, is to provide an anode chamber where the pressure gradient matches that in the cathode chamber (in this case with a slight flow from the anode to cathode chamber). It should be noted that for cells without this matching pressure gradient the force on the diaphragm

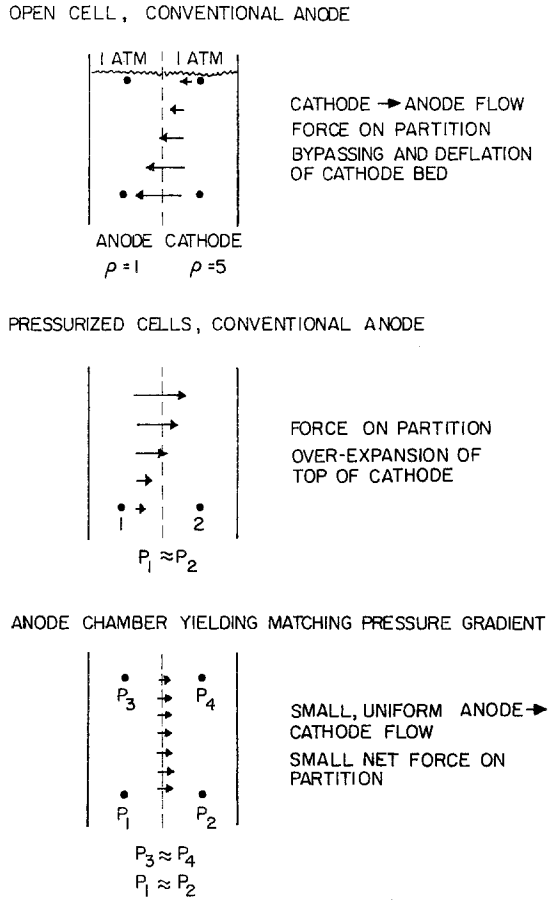

Fig. 1. Fluidized-bed cell flow configurations.

will increase, on scale-up, as the cube of the cell dimensions.

Arrangements tried in this investigation included fluidized- and packed-bed anodes, which have the advantage of providing a matching pressure gradient; the use of single and double layers of catalytically coated titanium mesh together with high anolyte flow rates; use of cloth-covered anodes placed directly in the fluidized cathodes, and the use of alternative anode reactions that do not involve gas bubbles in the anode chamber (such as the oxidation of dissolved sulphur dioxide). These various ideas were tested, either alone or in combination.

2. General description of experimental apparatus and procedure

The cell designs used in this investigation were variations on the basic cell depicted in Fig. 2. The

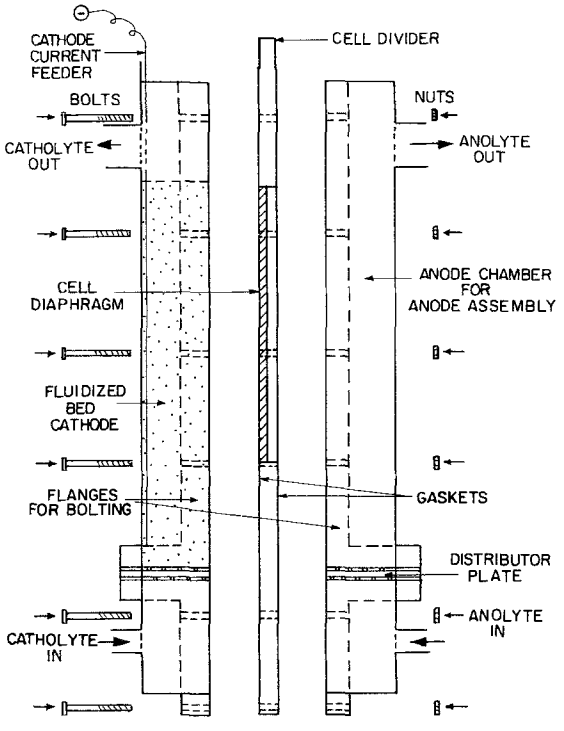

Fig. 2. Exploded view of rectangular fluidized-bed cell.

cell is made of plexiglass, in two halves, and is rectangular in cross-section. The inside dimensions of each half were 400 mm in height x 20 mm x 57 mm in the direction perpendicular to the paper. The wall dividing each half was 6.4 mm thick and contained a window (52 mm x 196 mm high) to hold the cell diaphragm. The bottom of the window was 80 mm above the distributor plate which consisted of two layers of phenolic plastic separated by 2.4 mm and drilled with 0.8 mm holes on 8 mm centres. The diaphragm, in most instances of a material called 'Daramic' supplied by W. R. Grace Co., was glued into the window so that it was flush with the dividing wall on the cathode side. The cathode was usually operated so that it was 280 mm high in the fluidized state. Anolyte and catholyte left through ports in the upper part of the cell. The two halves of the cell were bolted together using neoprene gaskets or a silicon sealant. The cathode consisted of cleaned, 24 x 35 mesh, cut wire, copper particles. The cathode current feeder was a flat copper sheet glued to the back of the cathode compartment and extending from the distributor plate through the top of the cell.

The electrolyte flow system used in most of the experiments was based on that depicted in Fig. 3. Six cubic decimetres of electrolyte were used, 6 dm^3 of each in the case of separate anolyte and catholyte. Anolyte and catholyte were pumped from the reservoir(s), through the cell and overflowed back into the reservoir(s). Temperature control was achieved manually using electrical heaters and ice packs immersed in the reservoir(s). Current was supplied either by a Hewlett Packard 2621B power supply or by a transformer–rectifier–powerstat system built in-house. Cell voltage and current were recorded on a strip chart machine.

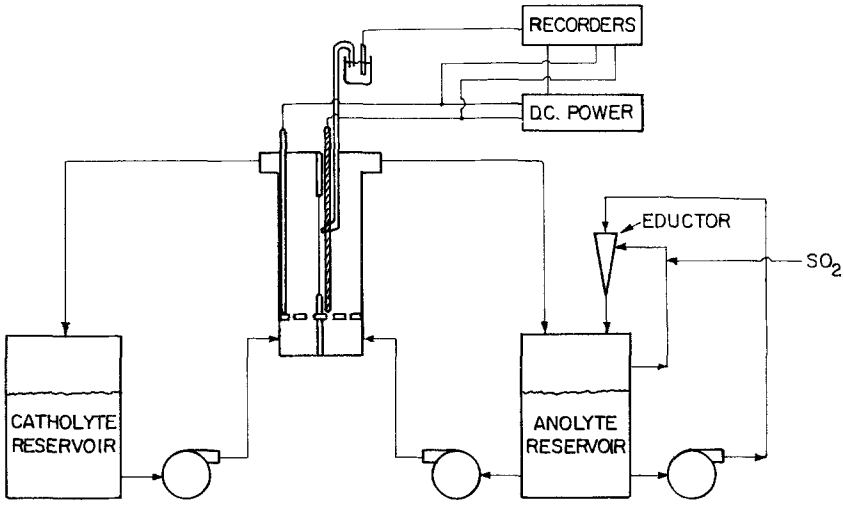

Fig. 3. Supporting equipment for fluidized-bed cell.

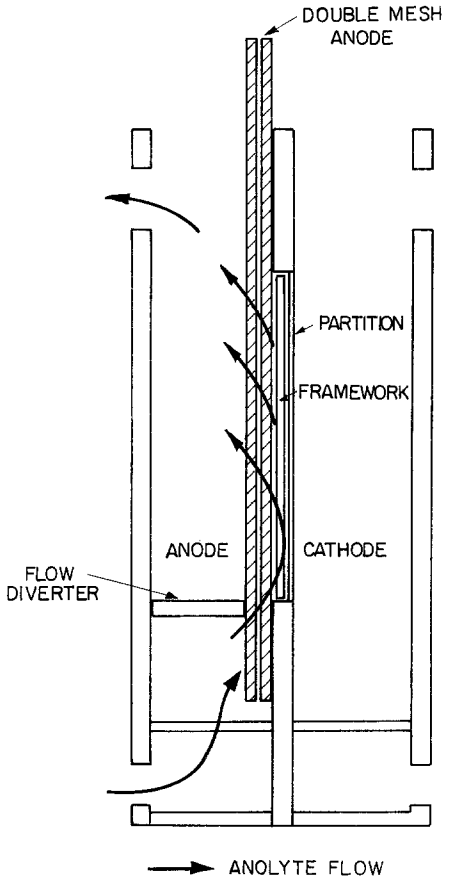

Fig. 4. Cell with double-mesh anode showing flow configuration.

The experimental procedure involved filling the electrolyte reservoir(s), turning on electrolyte pumps and bringing the electrolyte up to temperature. Particles were poured into the cathode chamber and the electrolyte flow momentarily turned off to establish the bed height in the collapsed state. After refluidizing the bed to the correct expansion a small sample of electrolyte was taken and the current turned on. Samples were taken throughout the run and copper contents determined by titration with sodium thiosulphate in acid solution using potassium iodide/starch indicator.

3. Particular anode systems

3.1. *Fluidized-bed anode*

This anode consisted of titanium particles (35 x 100 mesh) which had been given the same DSA catalytic coating by Diamond Shamrock Corporation as the anodes used in previous work at Berkeley. The anode current feeder was an expanded titanium mesh with the same coating. The anode distributor was of Nylon filter cloth stretched over a frame.

3.2. *Packed bed*

Packed-bed electrodes were made of 5 mesh, 4% antimonial lead shot or of graphite. The former was made by pouring the shot into the anode chamber without compaction; a current feeder of lead sheet was used. The latter was of 6 x 12 mesh, synthetic graphite.

3.3. *Double titanium mesh anode*

Two layers of Diamond Shamrock expanded titanium mesh, coated on both sides, were placed together close to the cell partition (see Fig. 4). A flow diverter placed in the anode chamber at the bottom of the diaphragm was designed to divert flow up along the double mesh. The diaphragm was supported by a framework of plexiglass placed between the diaphragm and anode. To provide additional support for the diaphragm, the cell top was sealed so that the anode chamber could be pressurized.

3.4. *Wrapped anodes*

Lead anodes, into whose surface a mesh of insulating material has been rolled, have been described in Canadian patents [15, 16]. The anodes are inserted directly into the bed and the insulating material serves as the diaphragm. A characteristic of such anodes is that the oxygen bubbles generated at the anode pass into the fluidized cathode. Two modified versions of this concept were tried at Berkeley. In the first a 19 mm square catalyst-coated titanium bar was wrapped with Nylon filter cloth secured with polyester thread. In the second a lead anode was wrapped with 100 mesh polyester screen cloth glued on the side away from the cathode current feeder and this anode was glued into the cathode side of the cell on the other side of the fluidized cathode from the current feeder.

3.5. *Alternative anode reactions*

The alternative anode reactions employed in this investigation were the oxidation of dissolved sulphur dioxide (with and without ferrous/ferric ions in solution) and the oxidation of cuprous ion in solutions containing acetonitrile. In the latter case the cathodic reaction was electrodeposition from conventional cupric-ion electrolyte in some tests and electrodeposition from the acetonitrile-stabilized cuprous-ion solution in another.

When sulphur dioxide was being used in the anolyte a separate pump continuously recirculated the anolyte from the bottom of the reservoir through an eductor and back to the reservoir. The gas input to the eductor was connected to the gas space of the anolyte reservoir and a source of SO_2 connected through a pressure demand regulator. In this way the anolyte was maintained at SO_2 saturation.

When cuprous ion was oxidized in the anode chamber a mat of copper, placed in the anode chamber, replenished the supply of cuprous ion. Additional information concerning apparatus and procedure can be found in the thesis [12] on which this paper is based.

4. Experimental results and discussion

The results presented here are, for the most part, in terms of cell voltage. The energy consumption per unit of metal deposited is proportional to this voltage and inversely proportional to the current efficiency. The latter is, in most instances, dependent on the configuration of the supporting apparatus since the primary cause of current inefficiency is attack of the copper particles by oxygen bubbles or dissolved oxygen carried from the anode chamber through the supporting apparatus and into the cathode chamber. It was found that by using separate anolyte and catholyte this attack could be virtually eliminated. Furthermore, by sealing the cathode side of the cell, and attaching a gas collection apparatus, the extent of hydrogen generation therein could be determined; no hydrogen was generated except at copper concentrations lower than those employed in the work reported here. It is conjectured that on an industrial scale the extent to which efforts would be expended to avoid this oxygen attack of the cathode (i.e. the current efficiency) would be determined by economic considerations. An exception to these generalizations is the case of wrapped anodes where the introduction of oxygen bubbles into the cathode bed is inherent in the anode design. For wrapped anodes the current efficiency was regarded as a significant variable.

4.1. *Fluidized-bed anodes*

Cell polarization curves for a cell using the fluidized anode and the standard electrolyte at room temperature appear in Fig. 5. Clearly this approach was not successful since the fluidized anode actually increased the cell voltage. The difficulty appears to be that the fluidized bed of coated titanium particles has a high effective resistivity compared to, say, a fluidized bed of copper particles. Table 2 reports the results of bed resistivity measurements made using the technique of Sabacky and Evans [17].

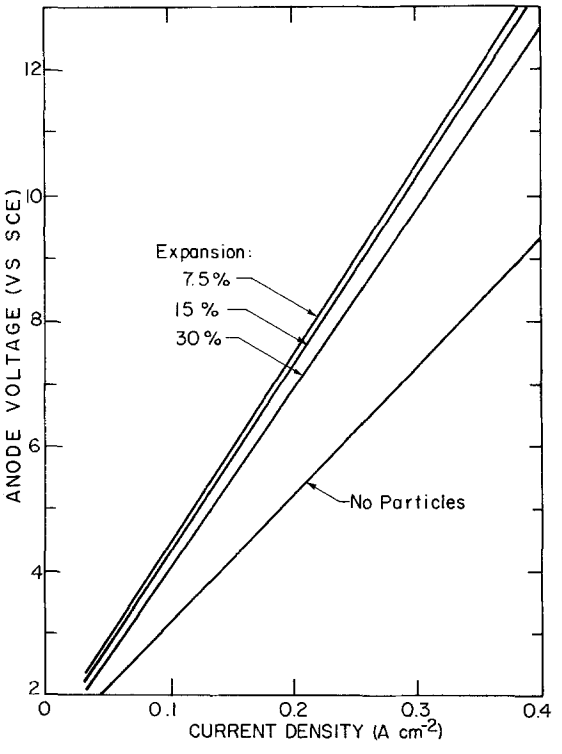

Fig. 5. Cell voltage versus current density for fluidized-bed anode system (25 g dm^{-3} Cu, 100 g dm^{-3} H_2SO_4, 50° C, regression line through the data).

Table 2. Resistivity of titanium or copper particle fluidized-bed

Bed expansion (%)	*Resistivity (Ω cm)*†	
	Ti	*Cu*
0	225	15.3
7	455	17.5
14	500	18.2

† Measured in 85.5 Ω cm H_2SO_4 electrolyte.

4.2. *Packed-bed anodes*

The packed bed of lead shot yielded excessive voltages (> 10 V at 0.43 A cm^{-2}) and inspection showed that only the one or two layers of shot next to the anode current feeder evolved oxygen. It is conjectured that high particle to particle contact resistance may have been responsible for this poor performance and alternative porous lead electrodes (e.g. of sintered shot) might be workable. This anode was effective in providing a pressure distribution in the anode matching that of the cathode.

The cell polarization curves for a packed bed of graphite particles evolving oxygen are shown in Fig. 6 for two different electrolyte temperatures. The curve for the 50° C electrolyte yields a cell voltage at 0.43 A cm^{-2} which is close to that for the conventional anode reported in Table 1. The anode is therefore seen to be comparable to a conventional one in terms of cell voltage and is superior in providing the desired anodic pressure gradient; cost and lifetime may be significantly different from those of the conventional anode.

4.3. *Double-mesh anodes*

Fig. 7 shows the cell voltage curves for the double-mesh anode evolving oxygen. Anolyte and catholyte, at 50° C, were separate with the former being sulphuric acid at various dilutions in water and the latter being the standard cupric electrolyte. The anode is appealing in that at 100% current efficiency the cell voltage at 0.43 A cm^{-2} corresponds to an energy consumption of 2.51 kW h kg^{-1} Cu, only a little above that of conventional copper electrowinning. It should be noted, however, that the double-mesh anode suffers from the disadvantage of not providing the desired pressure gradient within the anode chamber.

4.4. *Wrapped anodes*

The cell polarization curves for the wrapped titanium anode and the screen-covered lead anode appear in Fig. 8 (along with the curve for the

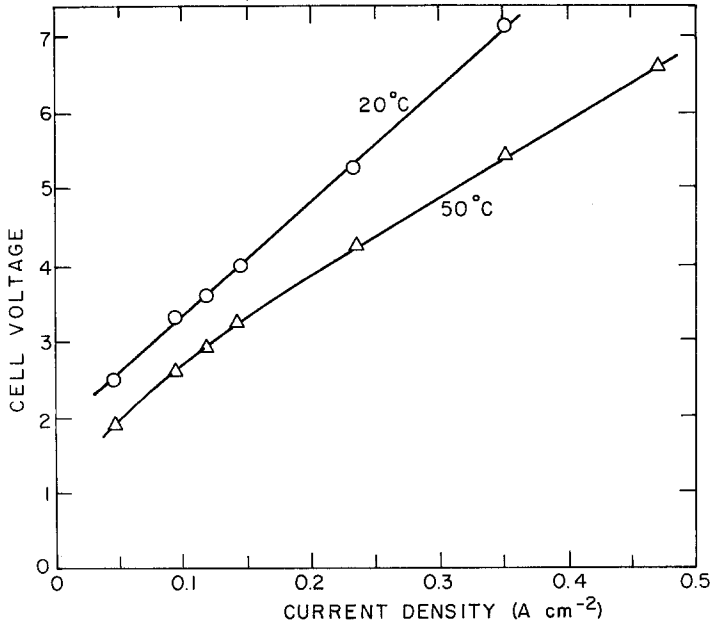

Fig. 6. Cell voltage versus current density for graphite packed bed evolving oxygen (25% cathode bed expansion, 50° C).

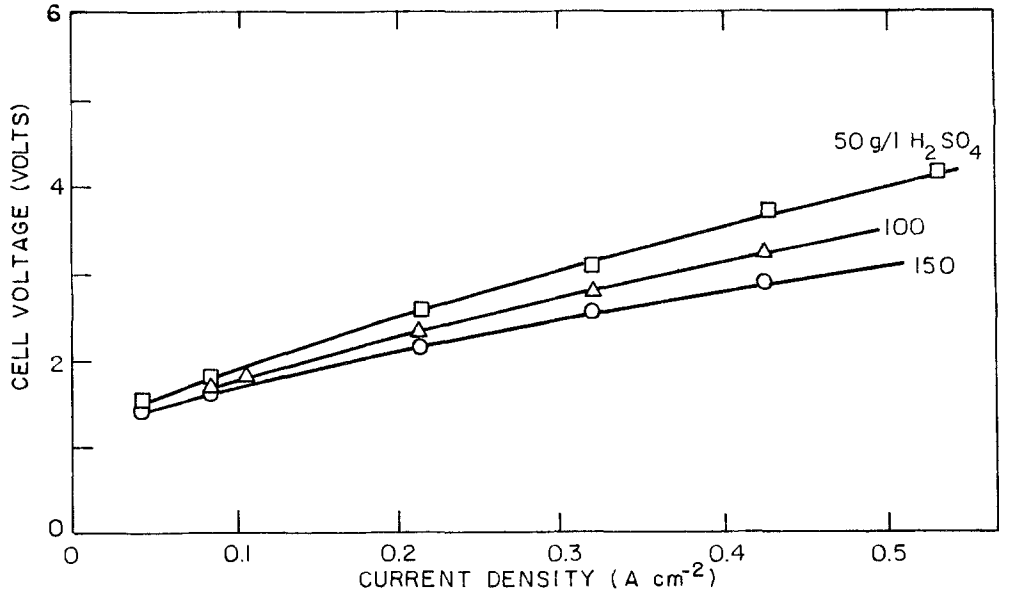

Fig. 7. Cell voltage versus current density for double-mesh anode at various anolyte concentrations of H_2SO_4 (25% bed expansion, 50° C).

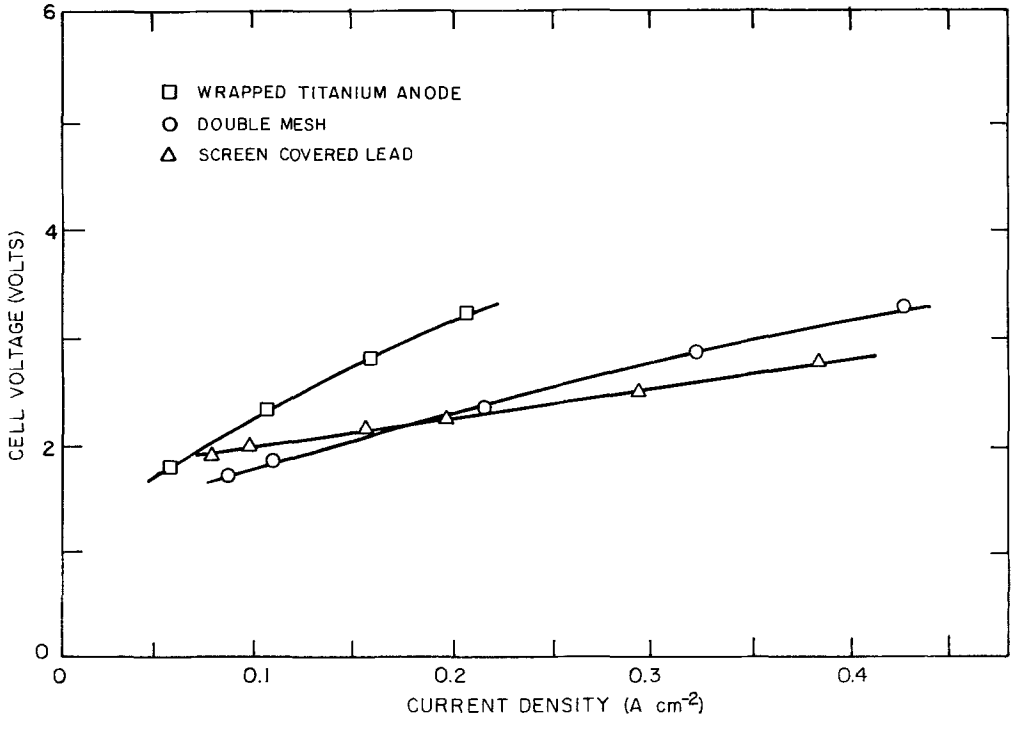

Fig. 8. Cell voltage versus current density for wrapped titanium anode and screen-covered lead anode (25% bed expansion, 50° C).

Table 3. Screen-covered anode: effect of temperature and current density on current efficiency and cell voltage

Current density (A cm^{-2})	Current efficiency (%)		Cell voltage (V)	
	30° C	50° C	30° C	50° C
0.5	60.6	50.9	3.15	2.89
1.0	70.0	63.4	3.4	3.5

double-mesh anode which has been reproduced here for comparison). The former was judged unsatisfactory becasue of high cell voltage, shorting by growth of copper through the Nylon and deterioration of this wrapping. The polarization curve for the screen-covered lead anode was encouraging in that it yielded a low cell voltage, lower than the double-mesh anode at high current density. However, oxygen bubbles generated at the anode have to pass through the fluidized bed before exiting the cell and this provides an opportunity for copper oxidation and current efficiency loss. A series of tests was therefore run to measure the effects of temperature and current density on cell voltage and current efficiency. The results are summarized in Table 3. Current efficiency values are based on a current efficiency calculation for each pair of successive electrolyte samples taken during a run. The cell voltage values have been averaged over each entire run.

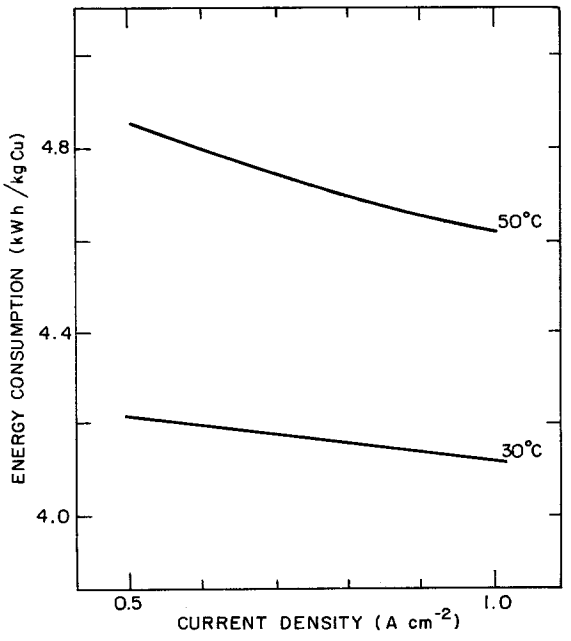

Fig. 9. Energy consumption versus current density for screen-covered lead anode (25% cathode bed expansion).

A linear regression analysis of the results of the current efficiency and voltage measurements appears as Fig. 9. Clearly the rather low current efficiency resulting from the wrapped anodes yields a relatively high overall energy consumption. It is conjectured that this problem would be compounded on scale-up; the residence time of an oxygen bubble would increase on scaling-up the bed height, giving a greater opportunity for the oxygen to re-oxidize copper.

4.5. *Alternative anode reactions*

So far, the discussion has been limited to the traditional case of oxygen evolution, a reaction which enjoys the advantages of a cheap reactant (water) and a product (H^+) that is readily used in the solvent extraction circuit upstream of electrowinning. The disadvantage of this reaction is that the oxygen bubbles significantly reduce the conductivity of the anolyte and thereby increase cell voltage. The oxidation of SO_2 as an alternative anode reaction in conventional cells has been examined by many previous investigators [e.g. 18, 19]. In most instances these investigators have used an anode with a catalytic surface (usually platinum). An alternative to a catalytic surface is to use ferrous ion as a depolarizer; this is oxidized at the anode to ferric ion which then reacts with SO_2 in the bulk of the solution, reforming ferrous ion. This latter approach has been used in the metallurgical industry to electrowin copper from leach solutions using carbon anodes [20]. The oxidation of SO_2 produces twice as much acid as the oxygen evolution reaction; this may be an advantage or disadvantage, depending on the overall acid balance of the copper plant.

In the present study, attempts to oxidize SO_2 were carried out on the Diamond Shamrock coated titanium mesh, in the form of a double layer, as described above, or in a packed bed of graphite particles, in the latter case with an electrolyte containing iron sulphate. In both cases the electrolyte contained 50 g dm^{-3} H_2SO_4 plus 12 g dm^{-3} SO_2, the SO_2 content being measured by titration with potassium permanganate. Fig. 10 gives the cell polarization results for the double-mesh anode

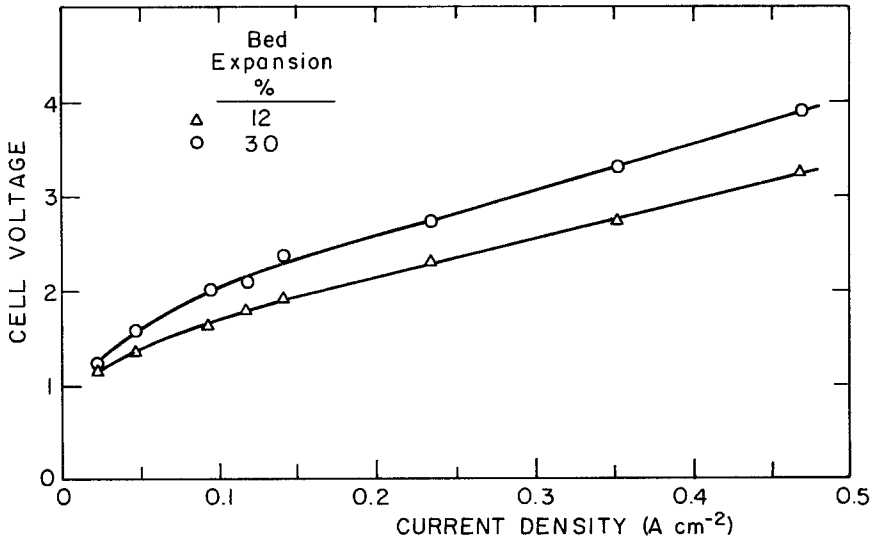

Fig. 10. Cell voltage versus current density for SO_2 oxidation on a double-mesh anode at 12% and 30% cathode bed expansion (50 g dm^{-3} H_2SO_4, 12 g dm^{-3} SO_2; 35° C).

at two different bed expansions of the cathode. The cell voltage was slightly lower than that obtained using the double-mesh anode alone. The anode generated oxygen despite the presence of SO_2 in solution and the rate of generation could be measured, enabling the current efficiency for SO_2 oxidation to be calculated. This anodic current efficiency is plotted in Fig. 11 where it is seen that the oxidation of SO_2 represents only a part of the anodic current at current densities of interest. These current efficiency measurements were made at an anolyte flow rate of 4.5 dm^3 min^{-1} resulting in an average superficial velocity of 6.6 cm s^{-1} past the mesh anode. The anolyte was resaturated with SO_2 after each measurement; the measurement took only a few minutes so there was no SO_2 depletion in the bulk of the anolyte.

Cell voltages for packed-bed oxidation of ferrous ion alone, at an iron concentration of 10 g dm^{-3}, and for oxidation in the presence of

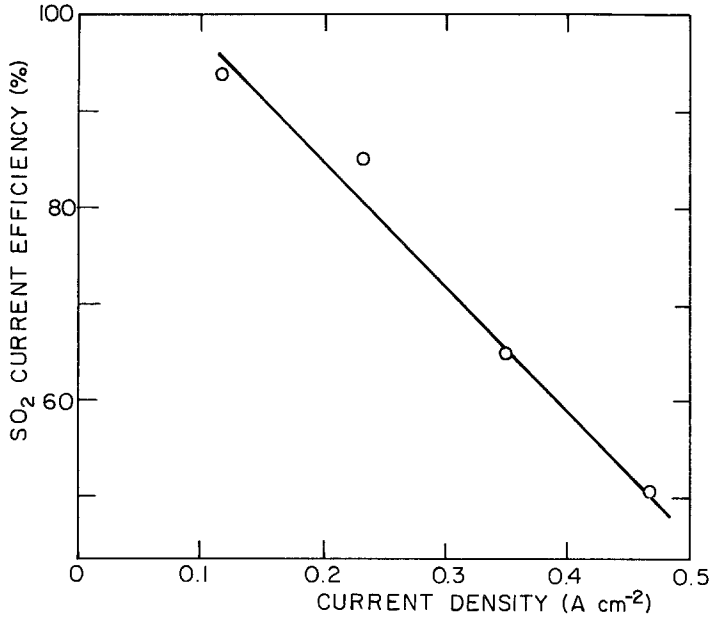

Fig. 11. SO_2 oxidation current efficiency versus current density for double-mesh anode (50 g dm^{-3} H_2SO_4, 12 g dm^{-3} SO_2; 35° C).

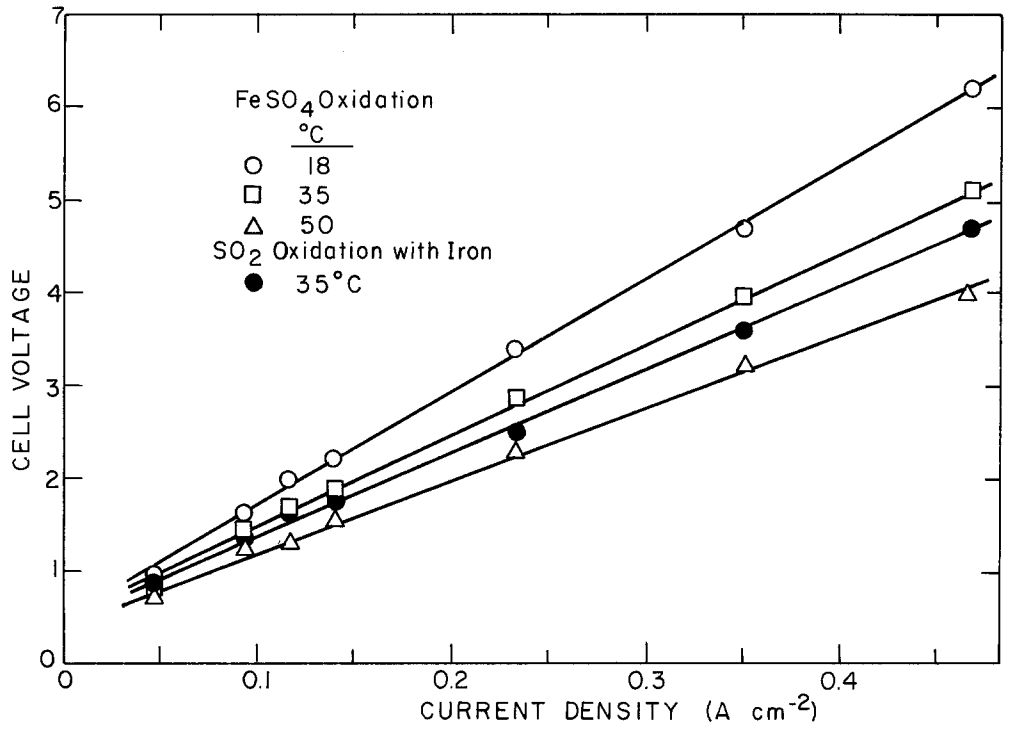

Fig. 12. Cell voltage versus current density for graphite packed bed using $FeSO_4$ anolyte and SO_2 (10 g dm^{-3} Fe, 50 g dm^{-3} H_2SO_4, 12 g dm^{-3} SO_2; 25% bed expansion).

SO_2 are reported in Fig. 12. The cell voltages are somewhat higher than with the double-mesh anode; no formation of oxygen bubbles was observed.

Another anode reaction of potential interest is the oxidation of cuprous ion, stabilized in aqueous solution by formation of the acetonitrile complex. Such an anodic reaction would require an auxiliary system for the reduction of the cupric ion formed at the anode; a chemical reduction, e.g. using hydrogen, is possible, while reduction by impure copper (cement copper) is an alternative which converts the plant to an electrorefining one. A related possibility is the use of cuprous ions in the catholyte as well as the anolyte. Further reduction in energy consumption may be possible in this way since only one electron is required for electrodeposition of each copper ion, versus two for cupric ion solutions.

In the investigations reported here the electrolyte contained 240 g dm^{-3} acetonitrile, 100 g dm^{-3} sulphuric acid and 20 g dm^{-3} copper. The standard catholyte was used in those runs where acetonitrile was present only in the anolyte. The graphite packed bed was used as the anode. Fig. 13 shows the cell voltages for the runs in which cuprous ions were used. No gas bubbles were observed in either the anode or cathode in these runs.

Table 4 provides a synopsis of the results of the test programme. The energy consumptions and cell voltages appearing in this table correspond to a superficial current density of 0.45 A cm^{-2}, a value thought to be appropriate for large-scale copper electrowinning.

5. Concluding remarks

The graphite packed bed is attractive from the point of view of providing the desired pressure distribution and large surface area for the anode reactions. Oxidation of ferrous and cuprous ions can proceed in this anode at high current efficiency and density. Development of better (more conductive) packed beds may make such anodes even more attractive. While the double-mesh anode yielded energy consumptions in the economic range, its drawbacks include substantial cost and the problem of partition support. Screen-covered lead anodes are simple but will suffer

Table 4. Summary of experimental results

	Cylindrical cell	*Graphite packed bed*					*Double-mesh anode*			*Screen-covered anode*
	Small anode	*Oxygen evolution*	*Cuprous anode*	*Cuprous anode plus cathode*	*$FeSO_4$ oxidation*	*SO_2 oxidation with $FeSO_4$*	*SO_2 oxidation*	*Oxygen evolution* (50 g dm^{-3} H_2SO_4)	*Oxygen evolution* (150 g dm^{-3} H_2SO_4)	*Oxygen evolution*
Temperature (°C)	50	50	50	50	50	35	50	50	50	30
Electrolyte resistivity (Ω cm)	3.0	2.53	4.25	4.25	5.1	6.1	4.5	4.6	2.5	3.0
Cell voltage (V) (at 0.45 A cm^{-2})	6.2	6.5	4.20	4.60	3.95	4.6	3.25	3.6	2.90	3.41 (at 1 A cm^{-2})
Energy consumption at 100% efficiency (kW h kg^{-1} Cu)	5.24	5.48	3.54	1.94	3.33	3.88	2.75	3.08	2.44	2.88
Current efficiency (%)	89	–	–	–	–	–	–	–	98	70
Energy consumption (kW h kg^{-1} Cu)	5.94	–	–	–	–	–	–	–	2.51	4.09

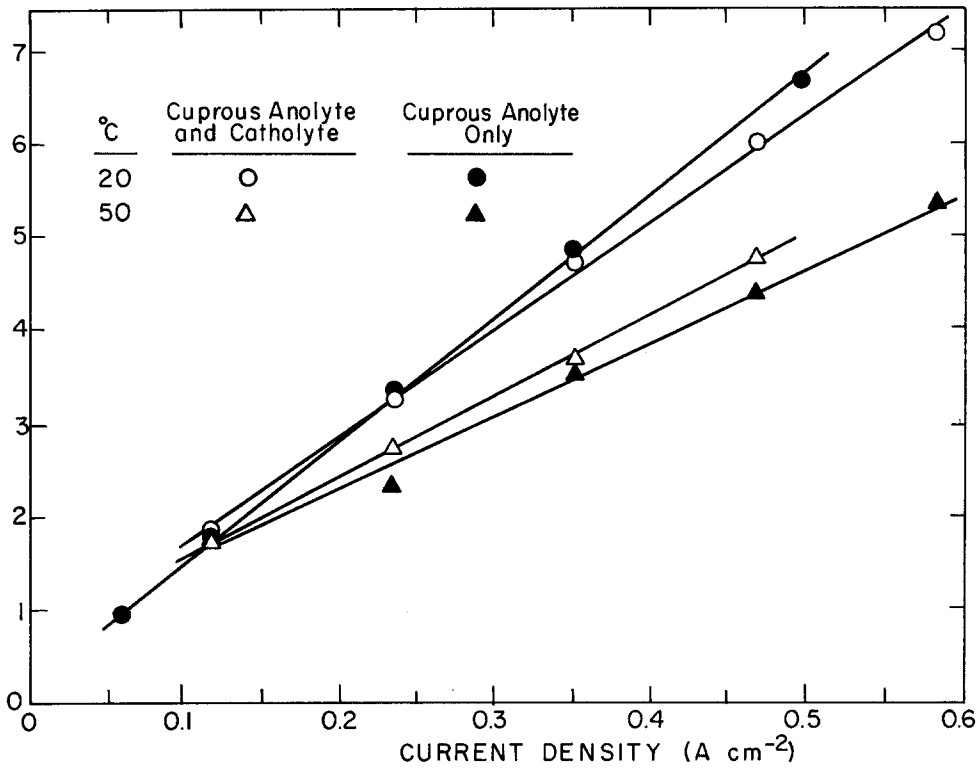

Fig. 13. Cell voltage versus current density for cuprous electrolysis in acetonitrile solution in a graphite packed bed (240 g dm^{-3} CH_3CN, 100 g dm^{-3} H_2SO_4, 20 g dm^{-3} Cu; 25% bed expansion, 50° C).

from high energy consumption unless the current efficiency problem associated with introducing oxygen into the fluidized cathode can be overcome. Lowest energy consumption was observed for the case where cuprous ions were used in both anolyte and catholyte. However, it should be recognized that this energy consumption, which is below that of conventional electrowinning, does not take account of any energy needs for the reduction of cupric ion to cuprous ion.

The results of this investigation are encouraging; even at this preliminary stage, the energy consumption associated with fluidized-bed electrowinning of copper has been substantially reduced by means which appear practical for large-scale industrial operations. A conclusion, as to which of these means for reducing energy consumption is the best, must await the results of further investigations and economic analyses of particular cases.

Acknowledgement

This research was carried out with support from the Office of Surface Mining through grant no. G5195006.

References

[1] D. S. Flett, *Chem. Ind.* **51** (1971) 300.
[2] *Idem, ibid* **16** (1972) 983.
[3] M. Fleischmann and G. M. Kelsall, *ibid.* **11** (1975) 329.
[4] A. J. Monhemius and P. L. N. Costa, *Hydrometallurgy* **1** (1975) 183.
[5] S. Germain and F. Goodridge, *Electrochim. Acta* **21** (1976) 545.
[6] C. C. Simpson, *J. Metals* **29** (1977) 6.
[7] M. Fleischmann, J. W. Oldfield and L. Tennakoon, *J. Appl. Electrochem.* **1** (1971) 103.
[8] J. A. E. Wilkinson and K. P. Haines, *Trans. Inst. Min. Met.* **81** (1972) C157.
[9] Bechtel Engineering to J. W. Evans, private communication.
[10] B. J. Sabacky and J. W. Evans, *J. Electrochem. Soc.* **126** (1979) 1176.

[11] *Idem, ibid* **126** (1979) 1180.
[12] D. P. Ziegler, MS thesis, University of California, Berkeley (1980).
[13] F. Hine, M. Yasuda, R. Nakamura and N. Toda, *J. Electrochem. Soc.* **122** (1975) 1185.
[14] I. F. Masterson and J. W. Evans, *Met. Trans. B* (1981).
[15] P. L. Claessens and J. L. Cromwell, Canadian Patent No. 996 500 (1976).
[16] N. R. Barucha and P. L. Claessens, Canadian Patent No. 1001 986 (1976)
[17] B. J. Sabacky and J. W. Evans, *Met. Trans. B.* **8B** (1977) 5.
[18] K. Wiesener, *Electrochim. Acta* **18** (1973) 185.
[19] E. T. Leo and D. T. Sawyer, *ibid* **10** (1965) 239.
[20] G. F. Pace and J. C. Stauter, *CIM Bull.* **1** (1974) 85.